

Height displacement sensing system based on varied period plane diffraction grating

WANG SHAN^{a,b}, ZHANG ZILI^{a,b,*}, MENG FANCHANG^a, WANG PENG^c

^aInstitute of Microelectronics of the Chinese Academy of Sciences, Beijing, 100029, China

^bUniversity of Chinese Academy of Sciences, Beijing, 100049, China

^cNanjing University of Aeronautics and Astronautics, Nanjing, 210016, China

A height displacement sensing system based on varied period plane diffraction grating fabricated by electron beam lithography method was proposed and demonstrated experimentally. The system is comprised of broadband light source, Y-type twin-core fiber, collimator lens, aluminium coating reflector, grating and optical stage. In the system, the designed grating line density was changed from 950 to 590 L/mm, and the grating size was 80 mm × 10 mm. When the height of optical stage changes, the light spot moved to different grating positions, and the diffracted light wavelength changed simultaneously. When the height displacement changed from 0 to 25 mm, the diffracted light wavelength changed from 1108 nm to 1328.62 nm with sensitivity of 9.39 nm/mm, and linearity of 0.996. Thus the height displacement can be deduced according to the wavelength of the diffracted light. The systematic error, gross error and uncertainty evaluation of the proposed height displacement sensing system were studied respectively. The error analysis of the system was executed which showed that the uncertainty the system is 0.110 nm.

(Received June 1, 2021; accepted November 24, 2021)

Keywords: Height displacement sensing, Varied period plane grating, Electron beam lithography, Uncertainty evaluation

1. Introduction

Plane grating was widely used in the applications of monochromators [1], X-ray grating spectrometer [2], spectral analysis [3], angle measurement [4], near-infrared polarization imaging [5], terahertz reflector [6,7] and so on, because of its advantages of fast response, compact structure and high diffraction efficiency. As one type of the plane grating, the varied period gratings have different grating line density at different grating positions [8], thus, it shows advantages such as flexible diffracted light wavelength, wide spectral region for optical sensing applications.

As one important optical component, the varied period plane grating fabrication techniques includes electron beam lithography (EBL) [9], holographic interference lithography [10], vacuum nanoimprinting process [11]. For the mentioned above grating inscription methods, the EBL fabrication technique has advantages such as special pattern production, high fabrication accuracy and flexible grating size [12-14]. The varied period plane grating (VPPG) based on EBL inscription method has been used for spectrum analyzer, optical filter, imaging, optical sensing. However, sensing characteristics of VPPG height displacement has not been studied.

In paper, a height displacement sensing system based on the VPPG inscribed by EBL combined with reactive ion etching (RIE) technique was proposed and experimentally demonstrated. The grating fabrication process was researched and its height displacement sensing characteristics were tested. The designed sensing system was mainly composed of plane grating, broadband light

source, Y-type twin-core fiber and spectrum analyzer. When the light spot was irradiated at different positions of VPPG surface through adjusting grating height, the collected diffracted light was changed simultaneously, thus, demonstrating the possibility for height displacement test. The proposed VPPG height displacement sensing system has flexible wavelength tuning range and high sensitivity, and which shows beneficial for applications such as building structural health monitoring, micro-displacement measurement and optical fiber sensing.

2. Operation principle

The principle diagram of the designed VPPG is shown in Fig. 1, the grating period d is composed of line width a and line spacing b . For the proposed grating, the line width a is fixed, and line spacing b is changed according to the line density function, thus, the grating period d is changed gradually. As shown in Fig. 1, the input light angle is θ_i , and diffracted light angle is θ_d . When the incident light spot is irradiated at different period positions of VPPG, the diffracted light wavelength is changed. The line density function L is expressed in Eq. (1), and X means the displacement change.

$$L = 950 - 7.5X_n + 0.0043X_n^2 + 4.2667 \times 10^{-5}X_n^3 \quad (1)$$

The relations of input and diffracted light angle θ_i and θ_d can be shown by equation $m\lambda = d(\sin\theta_i + \sin\theta_d)$, the diffracted light wavelength is λ , d means the

grating period and m is diffracted light order. When the input light irradiates through small incident light angle, when $m=1$, as shown in Fig. 1, the diffracted light is collected along the input light path. For the proposed grating, the θ_i and θ_d are set as 20° , fixed grating line width is 288 nm. As shown in Eq. (1), the initial line density is 950 L/mm, the line spacing is 764 nm; the final line density is 590 L/mm, and the line spacing is 1406 nm, thus, the grating period is changed. The diffracted light wavelength is changed as light spot irradiated at different grating period positions.

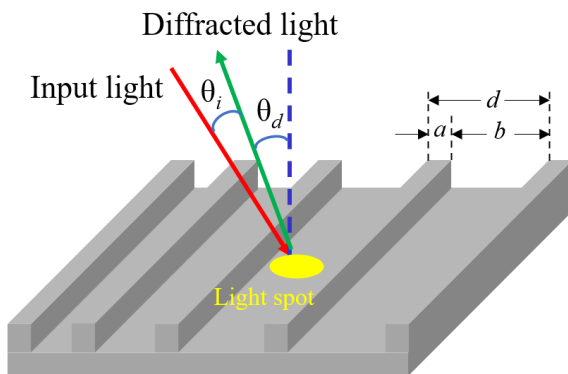


Fig. 1. Schematic diagram of the varied period plane grating (color online)

3. Materials and methods

The designed VPPG was fabricated by EBL combined with reactive ion etching (RIE) technique, the process schematic diagram is shown in Fig. 2, the quartz substrate was coated by aluminium and photoresist layer firstly; secondly, the photoresist layer was exposed by EBL line-by-line inscription technique, and the inscription region was 80×10 mm. After that, the RIE method was used for etching aluminium to generate grating pattern on the aluminium surface, and then, the photoresist layer was removed by acetone. Thirdly, the quartz was inscribed by RIE method to transfer aluminium pattern on the quartz surface. Finally, the quartz was coated an aluminium film by evaporation method. In the experiment, the proposed grating sample wafer and its optical micrograph observed by $60\times$ metalloscope are shown in Fig. 3 (a and b).

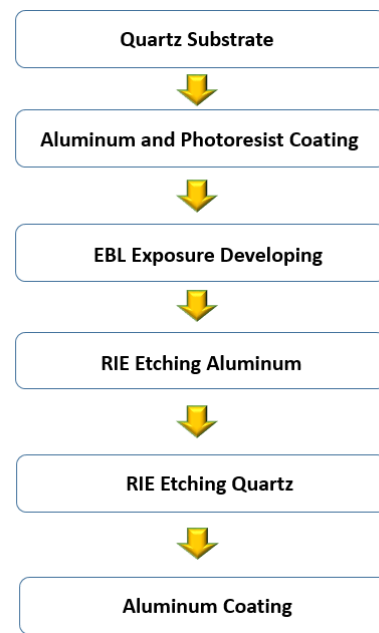


Fig. 2. VPPG inscription by EBL and RIE method process schematic diagram

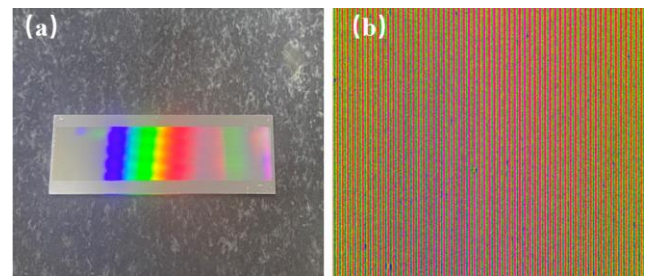


Fig. 3. (a) Fabricated VPPG wafer and (b) optical micrograph of the grating (color online)

The designed height displacement sensing system schematic diagram is shown in Fig. 4, the system is composed of broadband light source, Y-type twin-core fiber, collimator lens, aluminium coating reflector, grating and optical stage. One optical spectrum analyzer (OSA) is used to collect diffracted light. The broadband light is coupled into the Y-type twin-core probe with collimator lens, and light is irradiated on the reflector surface to transmit toward grating. The plane grating is placed on the optical stages of height direction tuneable. When the light is irradiated on the different positions of grating, the different diffracted light is generated due to its different grating period, and diffracted light is transmitted along the incident light path.

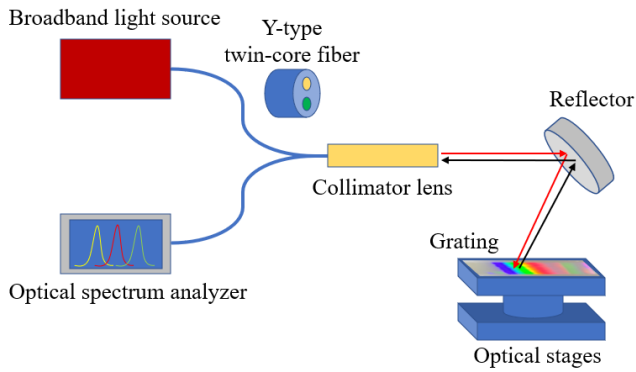


Fig. 4. Schematic of the VPPG height displacement sensing system (color online)

The diagram of varied period plane grating sensing is shown in Fig. 5. The incident light angle is fixed, as height displacement of optical stage is adjusted, the light spot on the grating surface is changed simultaneously and different diffracted light can be generated. As height displacement is increased, the light spot moves toward grating short period direction; on the contrary, the light spot moves toward grating long period direction gradually, and different diffracted light wavelengths can be realized.

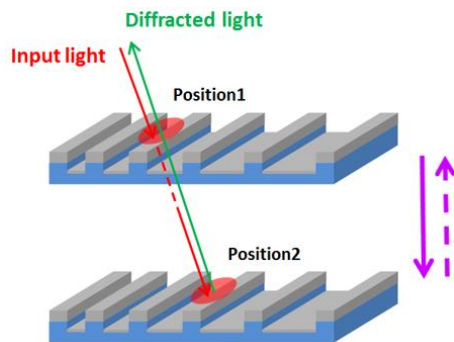


Fig. 5. Light path for different height displacement movement (color online)

4. Results and discussion

In the experiment, the sensing system was constituted, to improve the light efficiency and the quality of light spot, the diameter of the core was $600\mu\text{m}$, the incident light angle was 23° , the grating was placed on the optical stages, and the light spot was irradiated at the initial line density position 950 L/mm by adjusting the grating position, 660-nm diffracted light was collected. As shown in Fig. 6(a), when the light spot moved 1 mm along the plane grating transverse direction toward the long period position, the diffracted light shifted to 667.7 nm . After that, the light spot was irradiated around the grating low line density position through moving the grating, 1536-nm diffracted light was obtained, as shown in Fig. 6(b); when the light spot was moved 1 mm toward the grating long period direction, the diffracted light wavelength shifted to 1558.8 nm . Thus, the sensitivity of proposed VPPG was higher than 7.7 nm/mm .

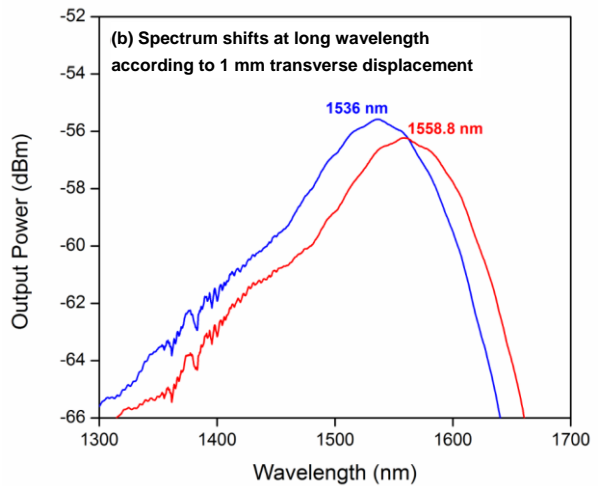
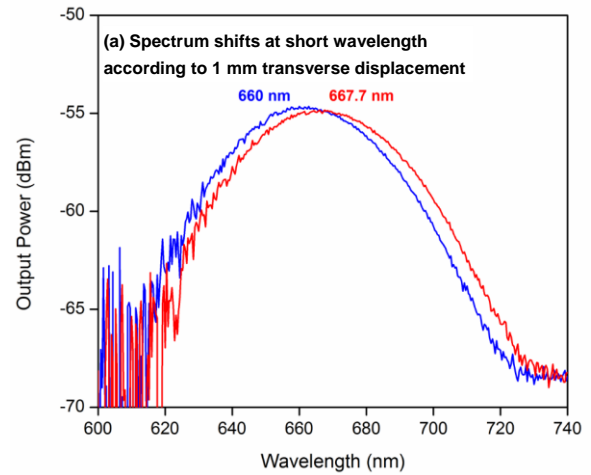


Fig. 6. 1-mm transverse displacement of VPPG. (a) light spot at high line density position and (b) light spot at low line density position (color online)

Then, the height displacement sensing characteristic was tested in the experiment. The distance between the grating and reflector mirror was adjusted by the optical stage. First, 1108 nm diffracted light was realized by adjusting the grating along the transverse direction, and then the grating and reflector mirror distance was increased from 0 to 25 mm in 5 mm by reducing the optical stage height. On the contrary, improving the height displacement would decrease the separation distance between reflector mirror and grating. The light spot moves from a short to a long grating period. As shown in Fig. 7(a), the diffracted light shifted in the long wavelength direction from 1108 to 1328.62 nm . Least squares fitting provided the height displacement sensitivity to be 9.39 nm/mm with linearity of 0.996 , as shown in Fig. 7(b), and the 3dB line width is direct proportional to the grating period. Thus, it can be found that the proposed VPPG-based height displacement sensing system demonstrates a flexible wavelength-tuning ability with high sensitivity.

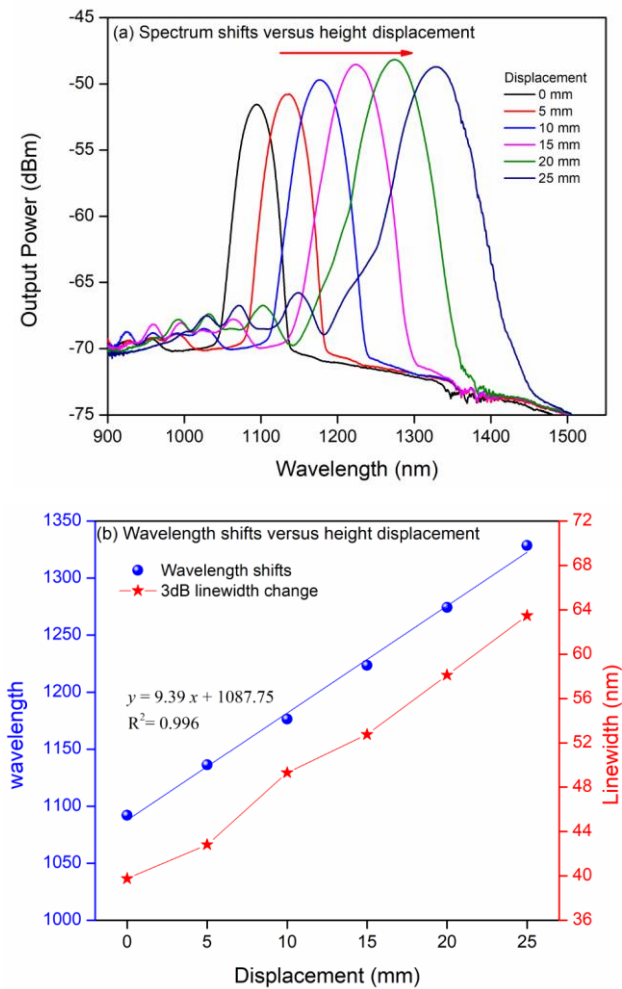


Fig. 7. VPPG wavelength shifts versus height displacement from 0 to 25 mm: (a) diffraction spectrum tuning procedure and (b) height displacement sensitivity and 3dB line width shifts (color online)

The repeatability of the proposed VPPG based height sensing system were test experimentally. For input light angle fixed at 23°, and 25-mm height displacement along the grating longitudinal direction, the diffracted light wavelength repeatability was as shown in Fig. 8, and the diffracted light wavelengths were superimposed during tuning procedure.

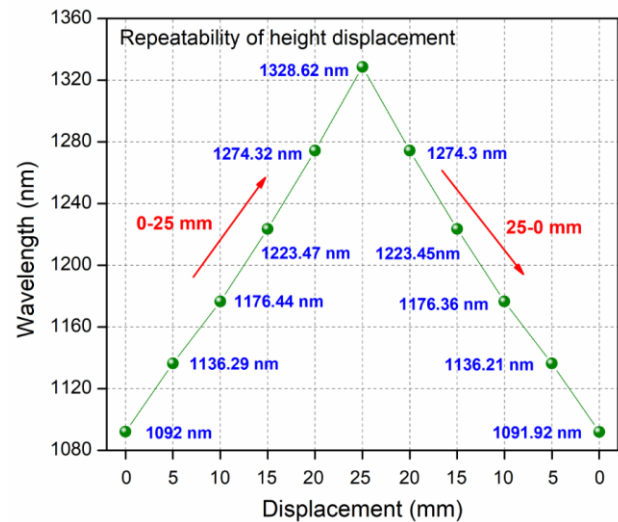


Fig. 8. Repeatability of proposed height sensing system (color online)

A set of measurements of the height displacement sensing system from 0 to 25 mm is as shown in Table 1.

Table 1. A set of measurements of proposed height sensing system at different height displacement

| Height displacement (mm) | Wavelength(nm) | | | | | | | | | |
|--------------------------|----------------|---------|---------|---------|---------|---------|---------|---------|---------|---------|
| 0 | 1092 | 1091.92 | 1092.07 | 1092 | 1092.07 | 1092 | 1092.04 | 1092 | 1092.05 | 1092.02 |
| 5 | 1136.29 | 1136.21 | 1136.21 | 1136.18 | 1136.21 | 1136.18 | 1136.18 | 1136.17 | 1136.21 | 1136.19 |
| 10 | 1176.44 | 1176.36 | 1176.44 | 1176.38 | 1176.44 | 1176.38 | 1176.39 | 1176.36 | 1176.42 | 1176.37 |
| 15 | 1223.47 | 1223.45 | 1223.41 | 1223.47 | 1223.41 | 1223.47 | 1223.38 | 1223.40 | 1223.39 | 1223.42 |
| 20 | 1274.32 | 1274.3 | 1274.27 | 1274.35 | 1274.27 | 1274.35 | 1274.24 | 1274.3 | 1274.25 | 1274.34 |
| 25 | 1328.62 | 1328.62 | 1328.62 | 1328.62 | 1328.62 | 1328.62 | 1328.57 | 1328.57 | 1328.60 | 1328.60 |

The residual error of the measurements was as shown in Fig. 9.

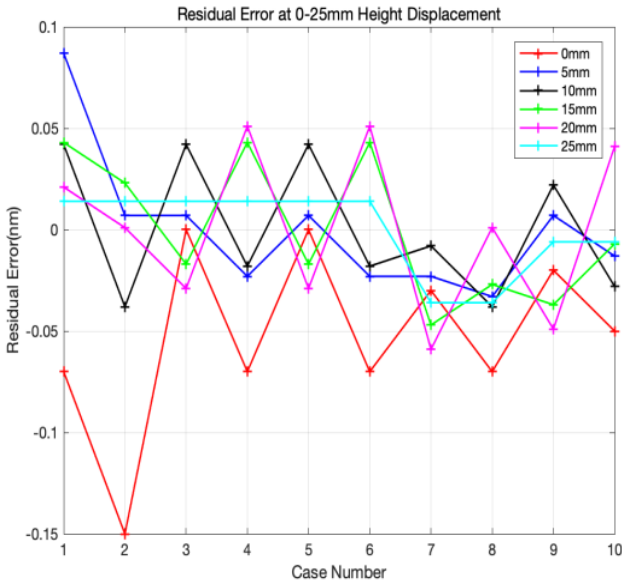


Fig. 9. Residual error of the measurements at 0-25mm height displacement (color online)

The results of measurements processing of the proposed height sensing system at 15 mm displacement, $n=10$ is as shown in Table 2, which is used to find the systematic error and gross error.

Table 2. The results of measurements processing of the proposed height sensing system at 15mm ($n=10$)

| i | λ_i/nm | v_i/nm | v_i^2/nm |
|-----|----------------|----------|------------|
| 1 | 1223.47 | 0.043 | 0.001849 |
| 2 | 1223.45 | 0.023 | 0.000529 |
| 3 | 1223.41 | -0.017 | 0.000289 |
| 4 | 1223.47 | 0.043 | 0.001849 |
| 5 | 1223.41 | -0.017 | 0.000289 |
| 6 | 1223.47 | 0.043 | 0.001849 |
| 7 | 1223.38 | -0.047 | 0.002209 |
| 8 | 1223.40 | -0.027 | 0.000729 |
| 9 | 1223.39 | -0.037 | 0.001369 |
| 10 | 1223.42 | -0.007 | 0.000049 |

$$\bar{\lambda} = \frac{\sum_{i=1}^n \lambda_i}{n} = 1223.427nm \quad v_i = \lambda_i - \bar{\lambda} \quad \sum_{i=1}^{10} v_i^2 = 0.01101nm$$

According to the Bessel formula and the Peters formula, the standard deviation can be calculated respectively in Eq. (2) and Eq. (3):

$$\sigma = \sqrt{\sum_{i=1}^{10} v_i^2 / 9} = 0.034 nm \quad (2)$$

$$\sigma' = 1.253 \times \sum_{i=1}^{10} |v_i| / \sqrt{10 \times 9} = 0.404nm \quad (3)$$

The standard deviation ration calculated by the two above methods can be stated as $\sigma'/\sigma = 1 + u$, since

$|u| = 0.15 < 2/\sqrt{n-1} = 2/\sqrt{9} \approx 0.67$. Therefore, there is no systematic error in the height displacement sensing system. Due to the small number of measurements, the Grubbs criterion can be used to determine whether the measurement results contained gross error. Arrange the measured wavelength values in order of magnitude, $\lambda_{(1)} = 1223.38nm$ and $\lambda_{(10)} = 1223.47nm$. According to the Grobs method, $g_{(10)}$ can be stated as $g_{(1)} = \bar{\lambda} - \lambda_1/\sigma = 1.382$, similarly, $g_{(10)} = \lambda_{(10)} - \bar{\lambda}/\sigma = 1.265$. From the Grubbs table, $g_0(10,0.05) = 2.18$, since $g_{(10)} < g_0$ and $g_{(1)} < g_{(10)}$. Therefore, there is no gross error in the height displacement sensing system.

The uncertainty in proposed height displacement sensing system can be addressed in accordance with the International Organization for Standardization Guide to the expression of uncertainty in measurement. The relationship between the height displacement (h) and the center wavelength (λ) can be described in Eq. (4):

$$h = 0.106\lambda - 115.841 \quad (4)$$

The standard uncertainty evaluated as type A is obtained from a series of measurements of center wavelength on the repeatability. Based on a set of measurements $n=10$, type A uncertainty u_1 can be calculated as $u_1 = 0.034/\sqrt{10} = 0.011 nm$. The most significant source of type B uncertainty in the sensing system is the resolution of the spectrometer, the corresponding standard uncertainty can be determined as $u_2 = 0.05/\sqrt{3} = 0.029 nm$. Therefore, in accordance with the ISO guide, the combined standard uncertainty $u_c(h)$ can be expressed as follows:

$$u_c(h) = \left[\left(\frac{\partial h}{\partial \lambda} \right)^2 u_1^2 + \left(\frac{\partial h}{\partial \lambda} \right)^2 u_2^2 \right]^{1/2} = 0.110nm \quad (5)$$

Thus, the uncertainty evaluation of the height displacement sensing system is 0.110 nm.

5. Conclusions

In the study, a height displacement sensing system employing with EBL inscribed varied period plane grating was proposed and experimentally demonstrated. For the designed plane grating, the grating size was $80 \times 10 mm$. As incident light spot was changed on the surface of grating, the diffracted light moved toward short and long direction respectively. For 0–25-mm height displacement adjustment, the diffracted light wavelength changed from 1108 to 1328.62 nm with sensitivity of 9.39 nm/mm, and linearity of sensing system was 0.996. The systematic error, gross error and uncertainty evaluation were study respectively, gross error and systematic error in the height displacement sensing system were not shown, and the uncertainty evaluation of the height displacement sensing system is 0.110 nm.

Acknowledgements

This research was supported by National Key Research and Development Project (grant number: 2019YFB2006700).

References

- [1] Z. Wang, X. Du, J. Hu, Q. Wang, P. Wang, Y. Tang, *Nucl. Instrum. Meth. A* **997**, 165150 (2021).
- [2] B. D. Donovan, R. L. McEntaffer, J. H. Tutt, B. C. O'Meara, F. Grise, W. W. Zhang, M. P. Biskach, T. T. Saha, A. D. Holland, D. Evan, J. Astron, *Telesc. Inst.* **7**(1), 104003 (2021).
- [3] Z. H. Yang, P. F. Li, Q. P. Fan, L. Wei, Y. Chen, *AIP Adv.* **10**(11), 115317 (2020).
- [4] S. Z. Tang, Z. R. Ren, Q. F. Han, W. F. Sheng, M. Li, *Rev. Sci. Instrum.* **91**(4), 045113 (2020).
- [5] D. Sun, B. Feng, B. Yang, T. Li, X. M. Shao, X. Li, Y. F. Chen, *Opt. Lett.* **45**(6), 1159 (2020).
- [6] B. Fang, S. Han, J. W. Xie, C. X. Li, Z. Hong, X. F. Jing, *Optoelectron Adv. Mat.* **13**(3-4), 175 (2019).
- [7] W. H. Zhu, B. Wang, H. T. Li, K. H. Wen, Z. M. Meng, Q. Wang, X. J. Xing, L. Chen, L. Lei, J. Y. Zhou, *Optoelectron Adv. Mat.* **12**(11-12), 629 (2018).
- [8] W. He, W. D. Zhang, F. Y. Meng, L. Q. Zhu, *Opt. Laser Eng.* **138**, 106456 (2021).
- [9] W. He, Y. H. Dong, L. Q. Zhu, M. L. Dong, *Results Phys.* **18**, 103193 (2020).
- [10] L. Qian, K. Wang, C. Han, *IEEE Photon. Technol.* **29**(11), 925 (2017).
- [11] J. Chen, W. Chen, G. Zhang, H. Lin, S. C. Chen, *Opt. Express*, **25**(11), 12446–54 (2017).
- [12] A. O. Kolesnikov, E. A. Vishnyakov, A. N. Shatokhin, E. N. Ragozin, *Quantum Electron.* **49**(11), 1054 (2019).
- [13] T. Shen, Z. Cai, Y. Liu, J. Zheng, *Appl. Opt.* **58**(24), 6622 (2019).
- [14] D. L. Voronov, E. M. Gullikson, H. A. Padmore, *Opt. Express* **26**(17), 22011 (2018).

*Corresponding author: zhangzili@ime.ac.cn